N_2S_2 Pyridinophane-Based Fluorescent Chemosensors for Selective Optical Detection of Cd^{2+} in Soils

Alessandra Garau,*[a] Larisa Lvova,*[b] Eleonora Macedi,*[c] Gianluca Ambrosi,[c] M. Carla Aragoni,[a] Massimiliano Arca,[a] Claudia Caltagirone,[a] Simon J. Coles,[d] Mauro Formica,[c] Vieri Fusi,[c] Luca Giorgi,[c] Francesco Isaia,[a] Vito Lippolis,[a] James B. Orton [d] and Roberto Paolesse [c]

a Dipartimento di Scienze Chimiche e Geologiche, Università degli Studi di Cagliari, S.S. 554 Bivio per Sestu, I-09042 Monserrato, Cagliari (Italy).
b Dipartimento di Scienze e Tecnologie Chimiche, Università di Roma "Tor Vergata", Via della Ricerca Scientifica 1, I-00133, Roma (Italy).
c Dipartimento di Scienze Pure e Applicate, Università degli Studi di Urbino "Carlo Bo", via della Stazione 4, I-61029 Urbino (Italy).
d UK National Crystallography Service, School of Chemistry, Faculty of Engineering and Physical Sciences, University of Southampton, SO17 1BJ, Southampton (United Kingdom).

E-mail: *agarau@unica.it*; *larisa.lvova@uniroma2.it*; *eleonora.macedi@uniurb.it*

Electronic Supporting Information
for
New Journal of Chemistry

Table of Contents

1. UV-Vis and fluorescence emission analysis

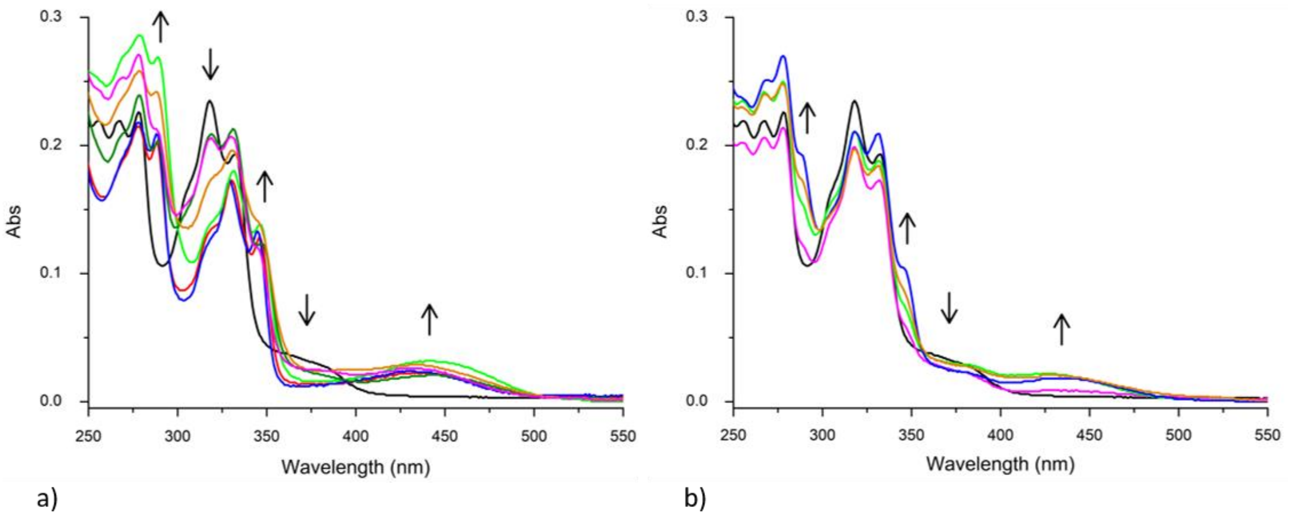

Figure S1. Absorption spectra of **L1** (black line) in the presence of a) 1 equiv. of Zn^{2+} (red line), Cd^{2+} (blue line), Ni^{2+} (green line), Cu^{2+} (magenta line), Co^{2+} (orange line) and Hg^{2+} (dark cyan line), and b) Pb^{2+} (magenta line), K^+ (green line), Mg^{2+} (blue line) and Fe^{3+} (orange line) ([**L1**] = $5.0 \cdot 10^{-6}$ M, MeCN/H_2O (4:1 v/v), pH 7.4, MOPS buffer $1.0 \cdot 10^{-2}$ M, 25 °C). Reported spectra were acquired either immediately after the addition for Zn^{2+}, Cd^{2+}, Cu^{2+}, Co^{2+}, Hg^{2+} or after one day for Fe^{3+}, K^+, Mg^{2+}, Al^{3+}, Ni^{2+} and Pb^{2+}.

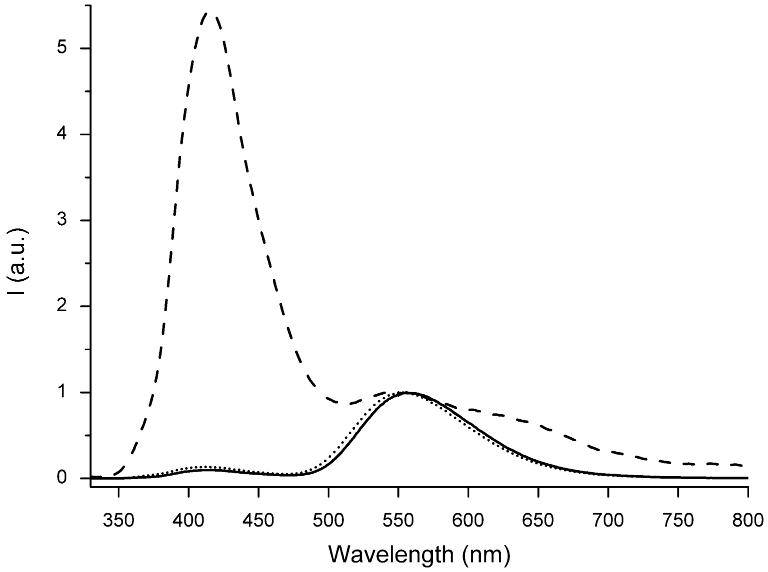

Figure S2. Normalised fluorescence spectra in the absence (dashed line) and presence of one equiv. of zinc (solid line) and cadmium (dotted line) ions ([**L1**] = $5.0 \cdot 10^{-6}$ M, MeCN/H_2O (4:1 v/v), pH 7.4, MOPS buffer $1.0 \cdot 10^{-2}$ M, 25 °C). Spectra are normalized to the intensity of the deprotonated form of the ligand (band at 558 nm).

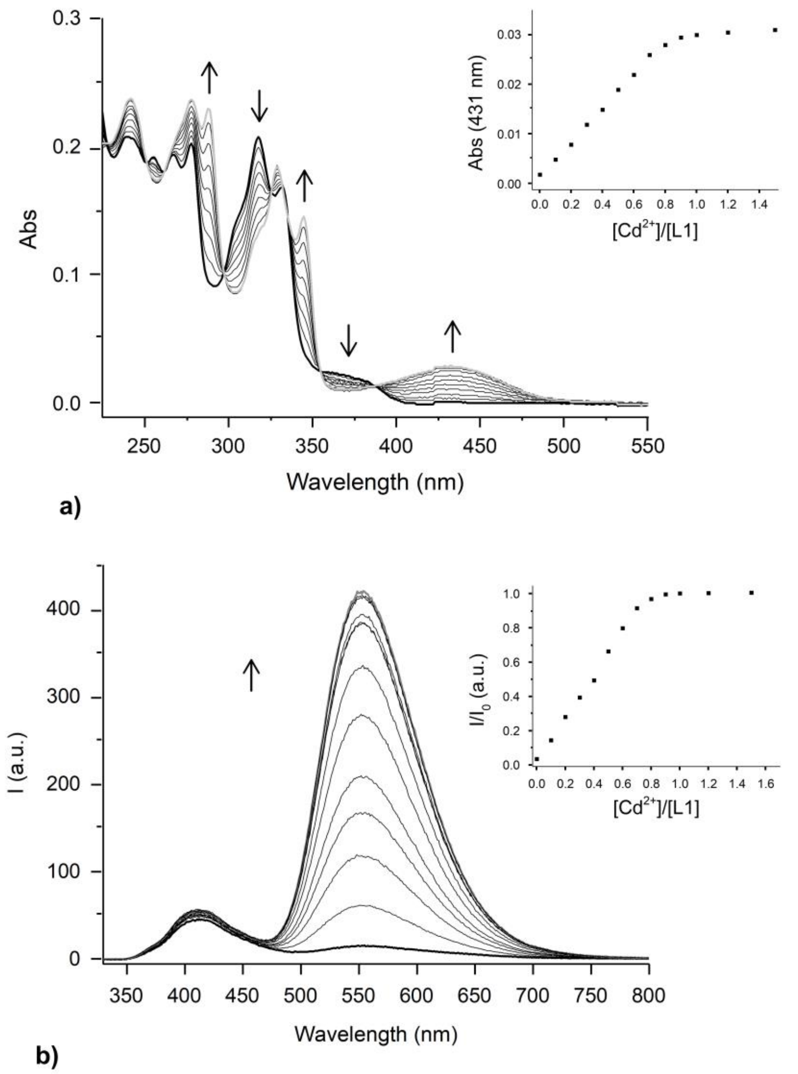

Figure S3. a) Changes in the UV-Vis spectrum of **L1** upon addition of increasing amounts of Cd^{2+}, inset: corresponding absorbance at 431 nm *versus* molar ratio plot; b) changes in the emission spectrum of **L1** upon addition of increasing amounts of Cd^{2+}, inset: corresponding normalized fluorescent intensity at 553 nm *versus* molar ratio plot ([**L1**] = $5.0\cdot10^{-6}$ M, MeCN/H_2O (4:1 v/v), pH 7.4, MOPS buffer $1.0\cdot10^{-2}$ M, 25 °C, λ_{ex} = 320 nm. Time elapsed between additions: 5 minutes).

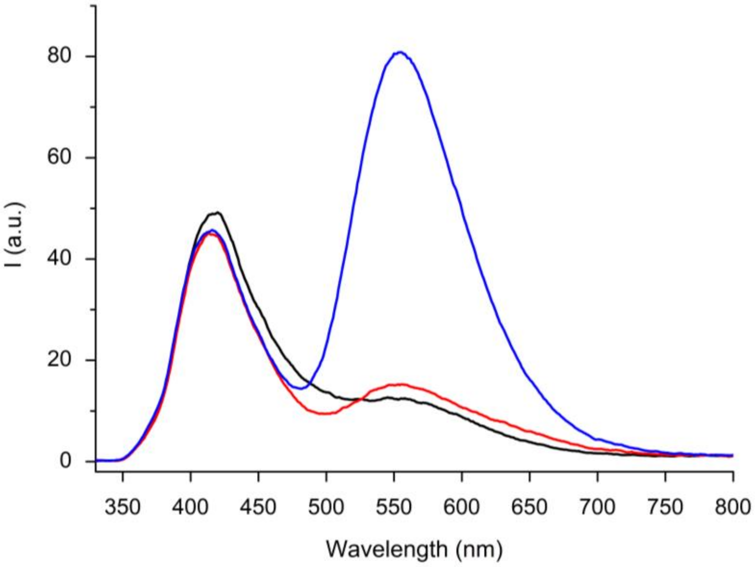

Figure S4. Emission spectra of **L1** at pH 2.13 (black line), 7.42 (red line) and in the presence of an excess of tetramethylammonium hydroxide (blue line) ([**L1**] = $5.0 \cdot 10^{-6}$ M, MeCN/H_2O (4:1 v/v), 25 °C, λ_{ex} = 320 nm).

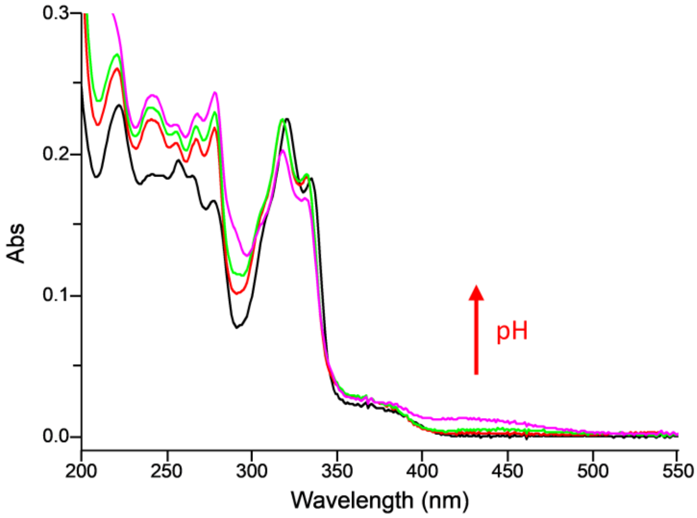

Figure S5. Changes in the UV-Vis spectrum of **L1** upon pH variation (pH 2.13: black line, pH 7.42: red line, pH 10: green line, excess of OH^-: magenta line) ([**L1**] = $5.0 \cdot 10^{-6}$ M, MeCN/H_2O 4:1 v/v).

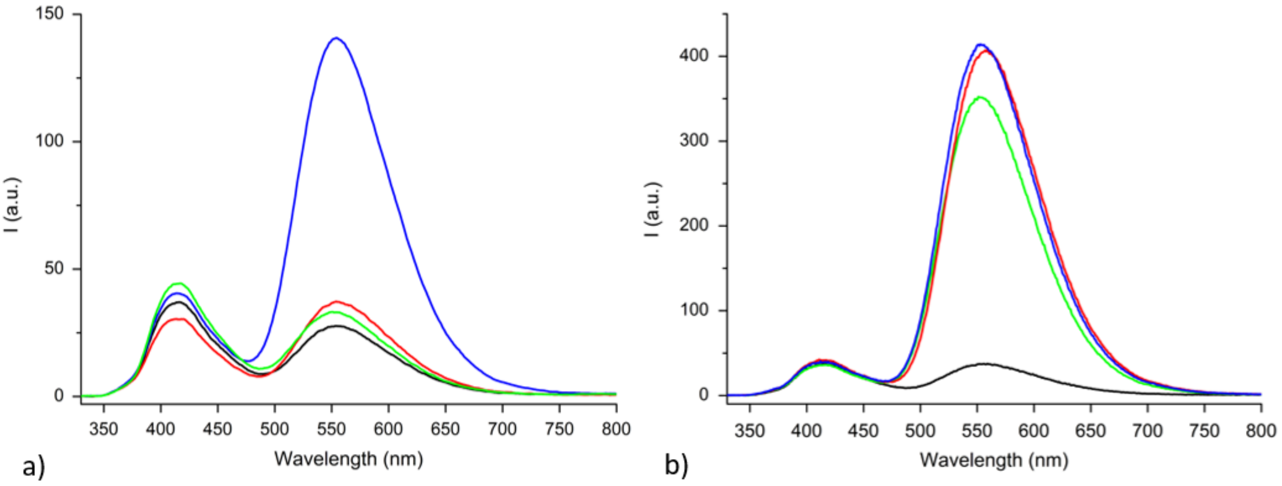

Figure S6. Changes in the emission spectrum of **L1** when adding the ligand to a mixture of 1 equiv. of a) all metal cations (Co^{2+}, Cu^{2+}, Fe^{3+}, Hg^{2+}, K^{+}, Mg^{2+}, Al^{3+}, Ni^{2+} and Pb^{2+}) (black line) or b) all metal cations except Hg^{2+} (black line), in the presence of 1 equiv. of Zn^{2+} (red line), 1 equiv. of Cd^{2+} (green line) or 1 equiv. of Zn^{2+} + 1 equiv. of Cd^{2+} (blue line) ([**L1**] = $5.0 \cdot 10^{-6}$ M, MeCN/H_2O (4:1 v/v), pH 7.4, MOPS buffer $1.0 \cdot 10^{-2}$ M, 25 °C, λ_{ex} = 320 nm).

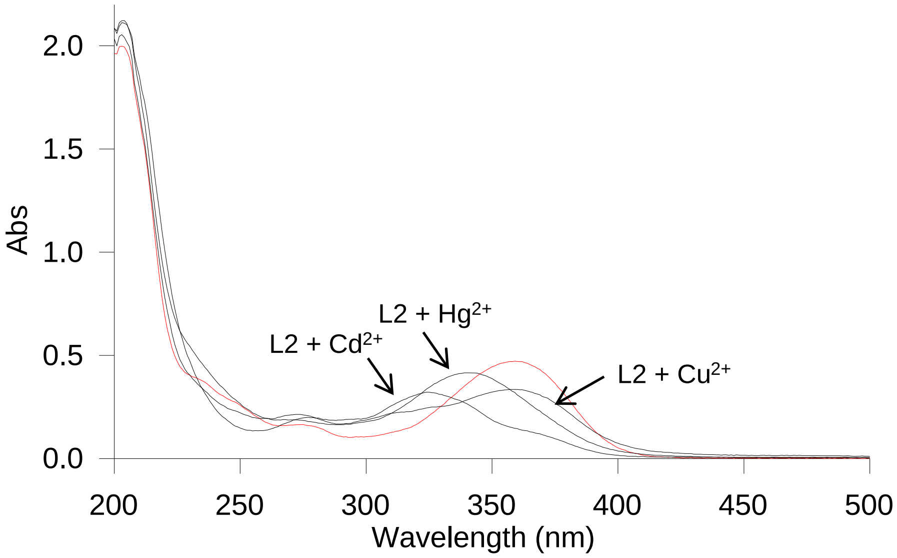

Figure S7. Absorption spectra of **L2** (red line) in the presence of 1 equiv. of Cd^{2+}, Cu^{2+} and Hg^{2+} ([**L2**] = $2.5 \cdot 10^{-5}$ M, MeCN/H_2O (4:1 v/v), pH 7.4, MOPS buffer $1.0 \cdot 10^{-2}$ M, 25 °C).

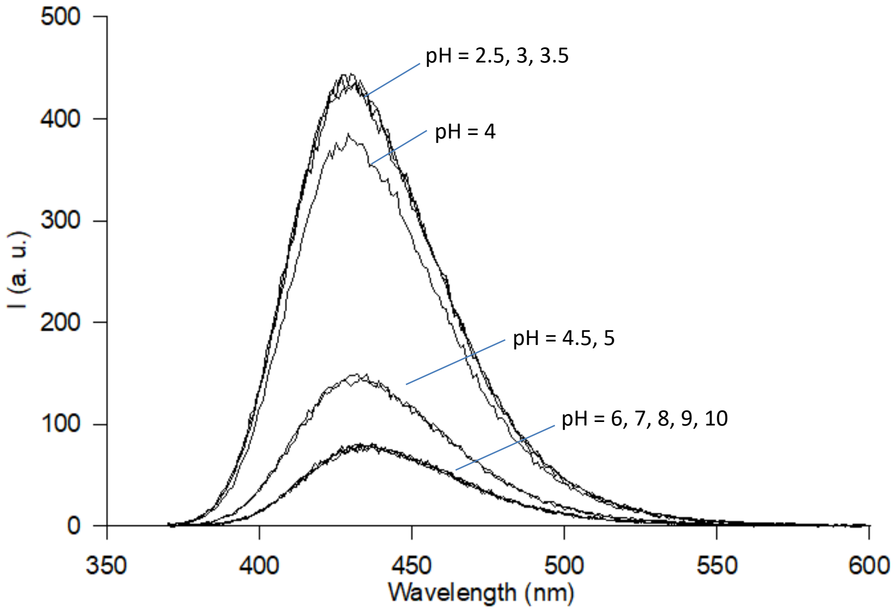

Figure S8. Emission spectra of **L2** at different pH ([**L2**] = 2.5·10^{-5} M, MeCN/H_2O (4:1 v/v)).

Ion competition studies additional data

Scheme S1. Different types of analysis performed on **L1** to study ion competition in MeCN/H_2O (4:1 v/v) at pH = 7.4 (MOPS buffer 1.0·10^{-2} M, 25 °C). a) Zn^{2+} added to an equimolar mixture of **L1** and M^{n+}; b) M^{n+} (5 equivs.) added to an equimolar mixture of **L1** and Zn^{2+}. Red sphere: Zn^{2+}; grey sphere: M^{n+} (M^{n+} = Cd^{2+}, Co^{2+}, Al^{3+}, Cu^{2+}, Fe^{3+}, Hg^{2+}, Ni^{2+}, Pb^{2+}, K^{+} and Mg^{2+}); white sphere: **L1**.

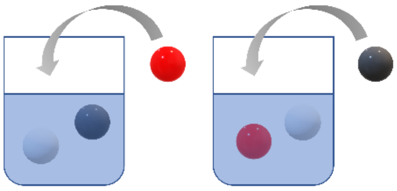

a) b)

Experimental section:

UV-Vis and fluorescence emission ion competition studies were performed also by adding 1 equiv. of **L1** to a mixture containing 1 equiv. of all metal cations, in the presence or absence of Hg^{2+}. Experiments were carried out in the presence of Hg^{2+} on:

- equimolar mixture of Co^{2+}, Cu^{2+}, Fe^{3+}, K^{+}, Mg^{2+}, Al^{3+}, Ni^{2+} and Pb^{2+};
- equimolar mixture of Co^{2+}, Cu^{2+}, Fe^{3+}, K^{+}, Mg^{2+}, Al^{3+}, Ni^{2+} and Pb^{2+}, in the presence of 1 equiv. of Zn^{2+};

- equimolar mixture of Co^{2+}, Cu^{2+}, Fe^{3+}, K^{+}, Mg^{2+}, Al^{3+}, Ni^{2+} and Pb^{2+}, in the presence of 1 equiv. of Cd^{2+};
- equimolar mixture of Co^{2+}, Cu^{2+}, Fe^{3+}, K^{+}, Mg^{2+}, Al^{3+}, Ni^{2+} and Pb^{2+}, in the presence of 1 equiv. of $Zn^{2+}$and 1 equiv. of Cd^{2+}.

Experiments were carried out in the absence of Hg^{2+} on:

- equimolar mixture of Co^{2+}, Cu^{2+}, Fe^{3+}, K^{+}, Mg^{2+}, Al^{3+}, Ni^{2+} and Pb^{2+};
- equimolar mixture of Co^{2+}, Cu^{2+}, Fe^{3+}, K^{+}, Mg^{2+}, Al^{3+}, Ni^{2+} and Pb^{2+}, in the presence of 1 equiv. of Zn^{2+};
- equimolar mixture of Co^{2+}, Cu^{2+}, Fe^{3+}, K^{+}, Mg^{2+}, Al^{3+}, Ni^{2+} and Pb^{2+}, in the presence of 1 equiv. of Cd^{2+};
- equimolar mixture of Co^{2+}, Cu^{2+}, Fe^{3+}, K^{+}, Mg^{2+}, Al^{3+}, Ni^{2+} and Pb^{2+}, in the presence of 1 equiv. of $Zn^{2+}$and 1 equiv. of Cd^{2+}.

2. NMR analysis

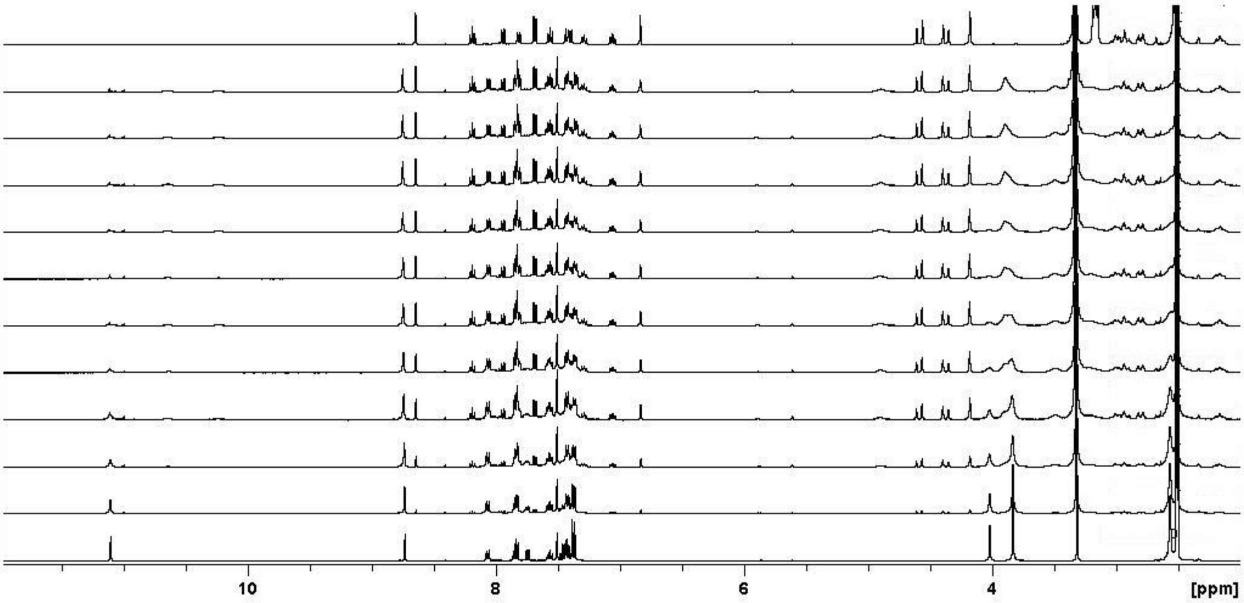

Figure S9. ^1H NMR titration of DMSO-d_6 solution of **L1** with Zn^{2+} ion. Zn^{2+} solution was added 0.1 equiv. at a time directly in the NMR tube; the tube was then kept for 10 min at 298.1 K before starting the acquisition of the spectrum. From bottom to top: **L1**, + 0.1-1.0 equiv. of Zn^{2+}, + 1 equiv. of NBu_4OH. [**L1**] = $1.0\cdot10^{-2}$ M, [Zn^{2+}] = $1.0\cdot10^{-1}$ M.

^1H NMR spectrum of **L1** in DMSO-d_6

The ^1H NMR spectrum of **L1** in DMSO-d_6 (Figure 9, bottom, main text) shows eleven aromatic and four aliphatic resonances, in addition to the -OH signal visible as a singlet at δ = 11.10 ppm and integrating for one proton (*H*25, s, 1H): a singlet at 8.73 ppm (*H*16, s, 1H), a doublet at 8.06 ppm (*H*21, d, 1H), a triplet at 7.84 ppm (*H*1, t, 1H), a doublet at 7.82 ppm (*H*18, d, 1H), a doublet of doublets at 7.74 ppm (*H*11, dd, 1H), a triplet of doublets at 7.56 ppm (*H*19, td, 1H), a singlet at 7.50 ppm (*H*23, s, 1H), a triplet at 7.46 ppm (*H*10, t, 1H), a multiplet caused by resonance overlap of multiple patterns at 7.42 ppm (*H*9+*H*20, 2H), a doublet at 7.37 ppm (*H*2, d, 2H), a singlet at 4.02 ppm (*H*7, s, 2H), a singlet at 3.83 ppm (*H*4, s, 4H). Finally, the last aliphatic resonance partially overlaps with the solvent peak at 2.57 ppm (*H*5+*H*6, m, 8H).

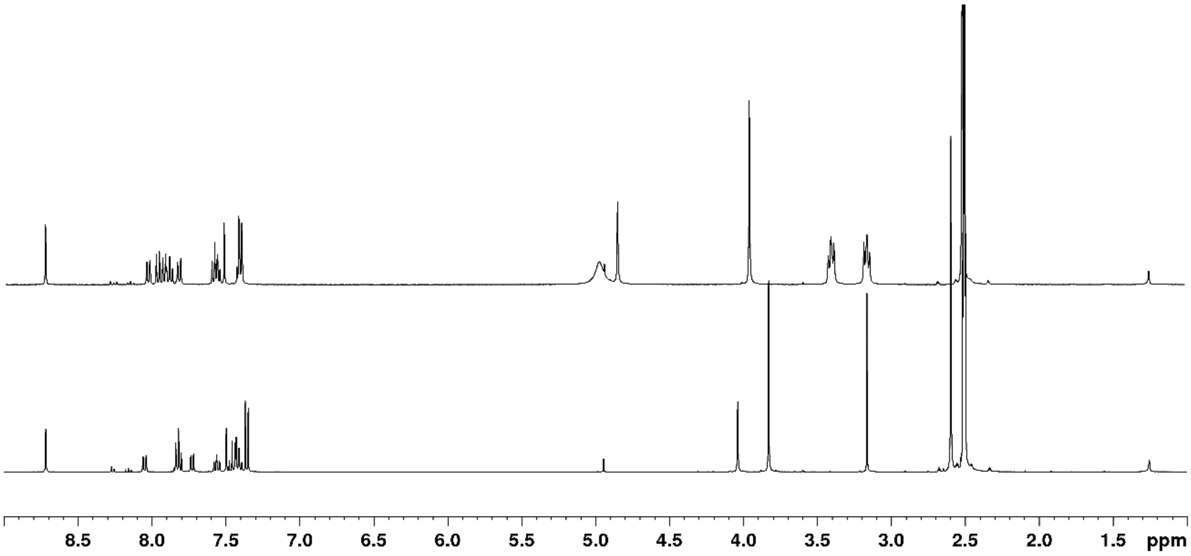

Figure S10. ^{1}H NMR spectra in DMSO-d_6 of free **L1** (bottom) and upon the addition of a drop of DCl [H**L1**]$^+$ (top).

^{1}H NMR spectrum of (H$_{-1}$**L1**)$^-$ in DMSO-d_6

Compared to the ^{1}H NMR spectrum of free **L1** in DMSO-d_6, the ^{1}H NMR spectrum of **L1** upon the addition of 1 equiv. of Bu$_4$NOH in the same solvent [(H$_{-1}$**L1**)$^-$, Figure S11, bottom] mainly shows a shift of the aromatic resonances, which are indeed more affected by the deprotonation of the naphtholic -OH group than the aliphatic resonances. The spectrum appears as follows: a singlet at 8.34 ppm (*H*16, s, 1H), a triplet at 7.83 ppm (*H*1, t, 1H), a doublet at 7.71 ppm (*H*21, d, 1H), a triplet at 7.60 ppm (*H*10, s, 1H), a doublet at 7.42 ppm (*H*18, d, 1H), a doublet at 7.37 ppm (*H*2, d, 2H), a doublet at 7.33 ppm (*H*9+*H*11, d, 2H), a triplet at 7.24 ppm (*H*19, t, 1H), a triplet at 6.98 ppm (*H*20, t, 1H), a singlet at 6.89 ppm (*H*23, s, 1H), a singlet at 4.00 ppm (*H*7, s, 2H), a singlet at 3.83 ppm (*H*4, s, 4H), a multiplet (overlapped to solvent peak) at 2.53 ppm (*H*5+*H*6, m, 8H).

The deprotonated form of **L1** (H$_{-1}$**L1**)$^-$ shows aliphatic resonances similar to **L1** (Figure 9a, main text), only *H5* and *H6* give a more complex system. Most HNBO signals undergo an upfield shift, in agreement with an increasing of the electron density following the deprotonation of the -OH group, while pyridine resonances stay unchanged.

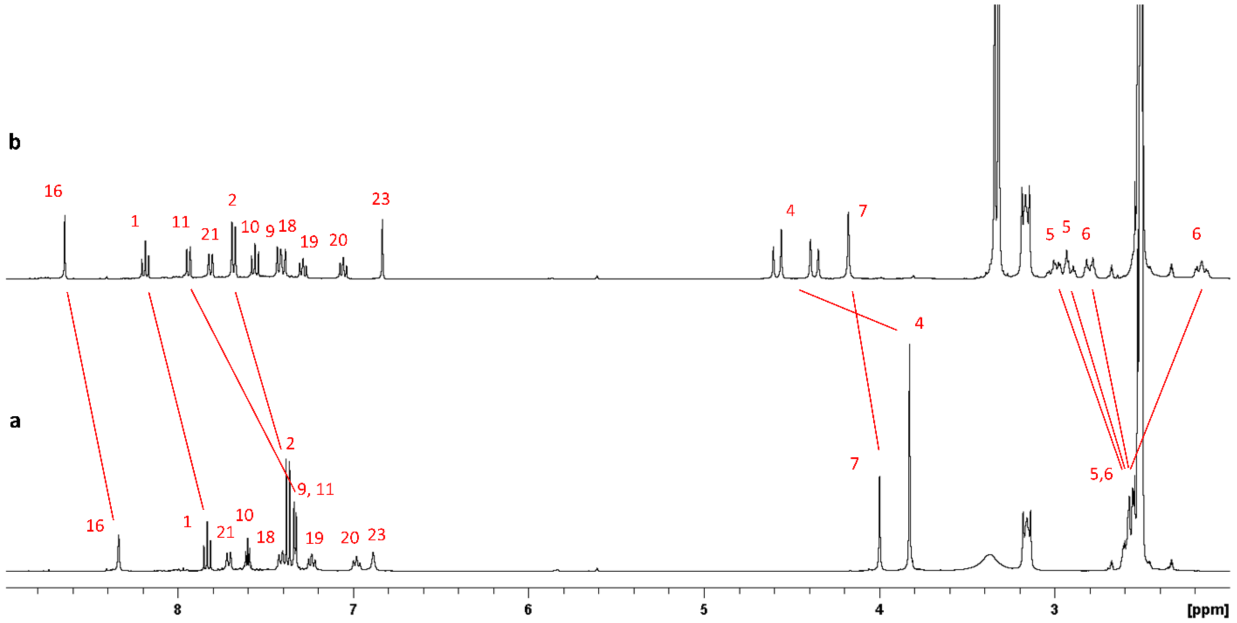

Figure S11. ^{1}H NMR spectra in DMSO-d_6 of deprotonated **L1**, $(H_{-1}\mathbf{L1})^-$ (1 equiv. of Bu_4NOH) (a) and in the presence of 1 equiv. of Zn^{2+} ion as perchlorate salt, $[Zn(H_{-1}\mathbf{L1})]^+$ (b). For the numbering scheme see Fig. 2 (main text).

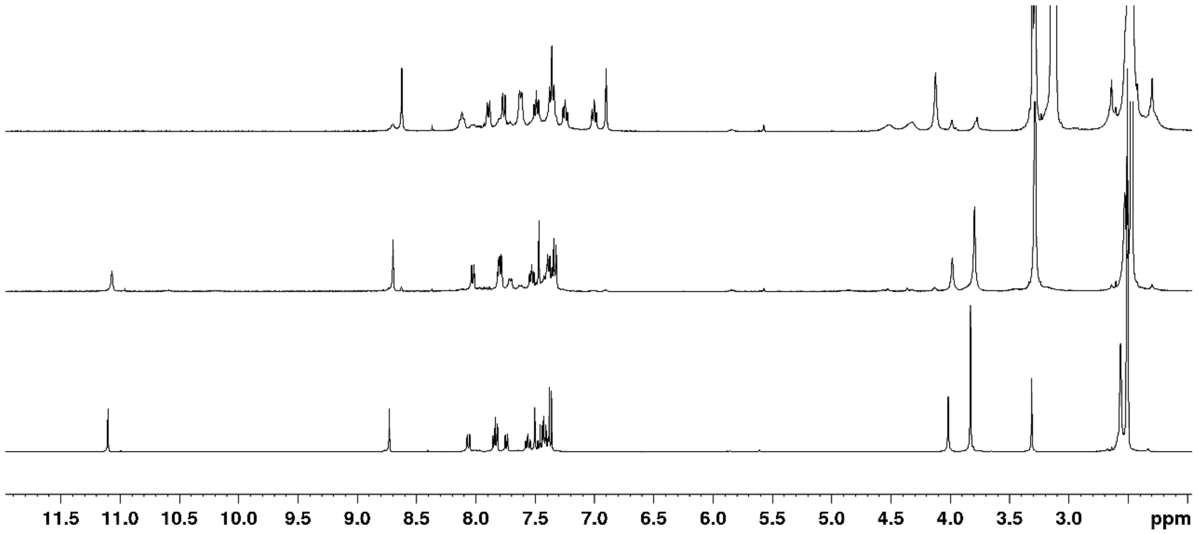

Figure S12. ^{1}H NMR spectra in DMSO-d_6 of free **L1** (bottom) upon sequential addition of 1 equiv. of Cd^{2+} ion (as perchlorate salt) (center) and 1 equiv. of Bu_4NOH (top).

Table S1. Resonance assignments (ppm) for free **L1**, its deprotonated form (H$_{-1}$**L1**)$^-$ and the [Zn(H$_{-1}$**L1**)]$^+$ complex (DMSO-d_6, 25 °C).

δ_{proton}	**L1**	(H$_{-1}$**L1**)$^-$	[Zn(H$_{-1}$**L1**)]$^+$	$\Delta\delta$ [a]
H1	7.84	7.83	8.19	0.36
H2	7.37	7.37	7.68	0.31
H4	3.83	3.83	4.37,4.58	
H5,H6	2.57	2.53	3.01,2.93 2.80, 2.16	
H7	4.02	4.00	4.18	0.18
H9	7.42	7.33	7.42	0.09
H10	7.46	7.60	7.56	-0.04
H11	7.74	7.33	7.94	0.61
H16	8.73	8.34	8.65	0.31
H18	7.82	7.42	7.40	-0.02
H19	7.56	7.24	7.29	0.05
H20	7.42	6.98	7.06	0.08
H21	8.06	7.71	7.81	0.10
H23	7.50	6.89	6.83	-0.06

[a] $\Delta\delta = \delta_{\mathrm{complex}} - \delta_{(\mathrm{H_{-1}\mathbf{L1}})^-}$

Table S2. Resonance assignments (ppm) for **L2** in the absence and in the presence of Cd^{2+} ion (CD$_3$CN/CDCl$_3$ (7:3 v/v), 25 °C).

δ_{proton}	**L2**	[Cd**L2**]$^{2+}$	$\Delta\delta$ [a]
H1	7.75	7.95	0.20
H2	7.37	7.58	0.17
H4	3.80	4.35,4.11	
H5,H6	2.51	3.16,2.79 2.56, 2.31	
H7	3.06	3.41	0.35
H8	2.66	2.89	0.23
H10	6.35	7.03	0.68
H13	5.87	6.12	0.25
H16	7.31	7.48	0.17
H17	6.51	7.05	0.54
H18	2.31	2.39	0.08
NH	5.14	6.01	0.87

[a] $\Delta\delta = \delta_{\mathrm{complex}} - \delta_{\mathbf{L2}}$

3. X-ray diffraction analysis

Table S3. Selected Bond Lengths (Å) and Angles (°) for **1.**

	Lengths (Å)
Cd1-N1	2.419(2)
Cd1-N2	2.532(2)
Cd1-O8	2.420(2)
Cd1-O14	2.584(2)
Cd1-O11	2.359(2)
Cd1-S1	2.6555(4)
Cd1-S2	2.6450(4)
	Angles (°)
N1-Cd1-N2	81.20(5)
N1-Cd1-O8	161.15(5)
N1-Cd1-O14	148.01(4)
N1-Cd1-S1	75.98(3)
N1-Cd1S2	77.50(3)
N1-Cd1-O11	97.98(5)
N2-Cd1-O14	87.80(5)
N2-Cd1-O8	102.00(5)
N2-Cd1-S1	79.33(3)
N2-Cd1-S2	77.16(3)
N2-Cd1-O11	161.42(5)
S1-Cd1-S2	146.784(14)
S1-Cd1-O8	122.84(3)
S1-Cd1-O14	72.49(3)
S1-Cd1-O11	82.46(4)
S2-Cd1-O8	85.06(3)
S2-Cd1-O14	129.15(3)
S2-Cd1-O11	120.96(3)

Table S4. Crystallographic Data for **1.**

Compound	**1**
Chemical formula	$C_{23}H_{27}N_5O_8S_2Cd$
Formula Weight	678.01
Space Group	*P*-1 (No. 2)
a/Å	8.16330(18)
b/Å	8.7604(3)
c/Å	19.2048(5)
α/°	96.042(2)
β/°	93.5240(19)
γ/°	109.789(2)
V/Å^3	1278.18(6)
Z	2
Z'	1
T/K	100(2)
λ/Å	0.71075
$D_{calc.}$/g cm^{-3}	1.762
μ/mm^{-1}	1.077
wR_2 (all data)	0.0568
wR_2	0.0563
R_1 (all data)	0.0229
R_1	0.0220